



## **Validation of Different Fan Modelling Techniques in Computational Fluid Dynamics**

Downloaded from: <https://research.chalmers.se>, 2026-04-03 10:07 UTC

Citation for the original published paper (version of record):

Franzke, R., Sebben, S. (2018). Validation of Different Fan Modelling Techniques in Computational Fluid Dynamics. Proceedings of the 21st Australasian Fluid Mechanics Conference, AFMC 2018

N.B. When citing this work, cite the original published paper.

## Validation of Different Fan Modelling Techniques in Computational Fluid Dynamics

Randi Franzke<sup>1,2</sup> and Simone Sebben<sup>1</sup>

<sup>1</sup>Department of Mechanics and Maritime Systems  
Chalmers University of Technology, Gothenburg, Sweden

<sup>2</sup>Volvo Car Corporation  
Gothenburg, Sweden

### Abstract

The accuracy of predicting the engine bay flow field with computational fluid dynamics (CFD) is crucial for designing efficient cooling systems for heat sensitive components. The engine cooling fan is the main driving component in cases of high thermal load, such as uphill driving with a trailer, or high speed driving on a highway, when the ram air itself is no longer sufficient for cooling purposes.

The most widely used fan modelling method is the Moving Reference Frame (MRF). This method can be used in steady and unsteady simulations, but has the drawback of using a fan geometry that is fixed in the global reference frame and, therefore, causing non-physical low velocity regions in the wake of the blades. The Rigid Body Motion (RBM or "sliding mesh") approach is a more accurate, but also more expensive approach, since it uses an unsteady solver. This study looks closely at the prediction of the flow field in the wake of an axial fan for different freestream velocities and fan speeds using the traditional MRF and RBM approach. In addition, a method that uses the average of flow field data for multiple MRF simulations with different fan positions is presented. Thereby the shadow of the fan blades is removed from the wake and the flow field becomes more uniform without the need of performing unsteady simulations. As a reference, measurements are performed on a vehicle fan with a 2D Laser Doppler Anemometry set-up in a small scale wind tunnel.

The results show good agreement between the measurements and the RBM simulations. As expected, the MRF simulations show a distinct blade pattern in the wake flow field. This was successfully removed by the proposed averaged MRF method. Even though there are still some differences between this method and the experimental results, the average MRF method has shown to be applicable as it improves the flow field results at a relatively low computational cost.

### Introduction

Electrified vehicles (EV) are currently the most promising solution for reducing CO<sub>2</sub> emissions in individual transportation. However, EVs contain more components that are sensitive to high heat inside the engine bay than a traditional vehicle with an internal combustion engine. Therefore more accurate tools to assess the thermal management are needed. One important issue is to predict the flow field under different load conditions, to ensure that hot and cold airstreams are transported to the appropriate locations. The main cooling fan is an important component for taking in and distributing cooling air to the engine bay, especially for high load cases that require additional cooling effort. Having a fan simulation model that gives the correct velocity magnitude and direction downstream of the fan is hence crucial in order to obtain a well predicted engine bay flow.

In the literature, multiple works can be found dealing with the measurement and simulation of fan flows. Khaled et al. [5] de-

signed a simplified engine bay with an industrial coolpack and used Laser Doppler Anemometry (LDA) and Particle Image Velocimetry (PIV) to measure the flow field between the fan and an obstacle representing the engine for different distances. However, this study was purely experimental and no comparison to numerical data was made. Gullberg et al. [1, 2] used the Moving Reference Frame (MRF) approach, to match CFD simulations to measured fan performance curves. However, these studies did not include an analysis of the flow field. Other experimental work was conducted by Kergourlay et al. [4] using constant temperature hot-wire anemometry to study the effect of different swept fan blades on flow structures and the energy spectrum. Similar work was done by Hurault et al. [3], who additionally compared experimental results to CFD data obtained by using the RANS model with Reynolds stress tensor turbulence modelling. However, the fan model was not specified. In their conclusions, the velocities were mainly found to be over-predicted due to the sensitivity of the measurement set-up. Measurements with Laser Doppler Anemometry on an axial fan have been used in noise prediction (aeroacoustics) of axial fans by Zenger et al. [7]. The most common approach in numerical aeroacoustic evaluation of fans is the usage of Large Eddy Simulation (LES) [7, 6]. For cooling performance and heat management cases, however, a simplified turbulence model is usually sufficient.

In this paper, the flow field resulting from the MRF and RBM model are compared with each other and with experimentally obtained data. Furthermore, another approach is presented that averages the flow field information over multiple MRF simulations and is, therefore, expected to improve the simulation results without adding considerable computational effort.

### Experimental Set-up

The Model Wind Tunnel (MWT) used for the experiments is a 1/5<sup>th</sup> scale version of the full-scale wind tunnel at the Volvo Car Corporation. The tunnel is of a closed-loop, slotted-wall type with a cross-section of 1.32 x 0.82 m<sup>2</sup>. For this study, however, the slots were taped over, creating a closed test section. This was done in order to facilitate the comparison with the simulation data. The test object is a Volvo V40 production fan with a diameter of 0.38 m, in its shroud. The fan is placed in the test section so that the fan rotation axis is in the centre of the wind tunnel cross section. Due to the asymmetry of the shroud, the space to the left and right of the shroud is not equally large. The set-up can be seen in Figure 1, with the LDA probe mounted on a yz-traverse downstream of the fan.

The investigated rotation speeds are 1400 rpm and 2800 rpm at a ram air flow of 5 m/s. The measurements are performed with a Laser Doppler Anemometry system by Dantec Dynamics. The probe is a 2D probe, with a focal length of 50 mm. In the set-up the probe is placed perpendicular to the flow to measure the  $u$  and  $w$  component of the flow in a yz-plane  $x=0.04$  m downstream of the fan's motor. The seeding is done with a battery

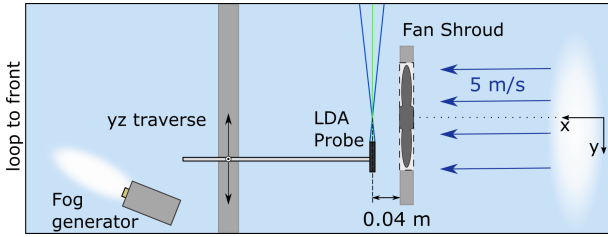


Figure 1: Experimental Set-up (top-view)

driven and remote controlled smoke machine, using a fog fluid on water-glycol basis. The fog generator is located downstream of the fan, to provide a more even seed particle distribution.

### Numerical Set-up

All simulations are performed with StarCCM+ (Ver. 11.06) from Siemens. The computational domain has the same cross section as the model wind tunnel. However, it is a bit longer than the test section, allowing the flow to settle. The mesh consists of  $8 \times 10^6$  polyhedral cells inside the fan domain and  $5 \times 10^6$  polyhedral cells in the remaining air domain. This yields a total of  $13 \times 10^6$  cells, and a  $y^+ < 1$  at the fan blades. A mesh dependency study was performed in which the area downstream of the fan was further refined, resulting in a total of  $23 \times 10^6$  cells. No significant changes in the flow field and the velocity contours could be observed.

Three different methods are used to model the fan rotation. First, the Moving Reference Frame (MRF) method is used. This model introduces a relative rotation to the respective user-defined region, while the fan blade geometry is fixed in the global reference frame. This model is commonly used, since it allows inexpensive steady-state simulations of rotation and/or translation. Second, the Rigid Body Motion (RBM) is studied. In this approach, the whole fan region is moving at the specified rotational speed. It is commonly recommended to use a time-step that represents a turn of less than 1 deg. Therefore, it is a very time consuming approach, but expected to give good results. The third method tested, is an averaged MRF approach. Since the fan is symmetric and has 8 blades, the geometry is repeating itself every 45 deg. Hence it is sufficient to cover this range by 9 simulations where the blade positions are changed by increments of 5 deg. A parametric study is conducted where the adaptation of this model to increments of 45 x 1 deg and 3 x 15 deg were tested. Starting from a converged standard MRF simulation, each new fan position required only 500 additional iterations before convergence was reached. The solution was considered to be converged, when all residuals of the governing equations decreased by two orders of magnitude and the maximum velocity stabilised.

The simulations based on the MRF methods were performed using a Reynolds-Averaged Navier Stokes (RANS) solver, using the realisable  $k-\epsilon$  turbulence model. The RBM simulations were performed with an unsteady RANS (URANS) solver, also using the realisable  $k-\epsilon$  model. For the comparison of RANS and URANS data, the URANS data is time-averaged over 10 fan revolutions.

### Results

In this section, the simulation results for all three methods are compared to measurement data that was taken 0.04 m downstream of the fan. The freestream velocity was 5 m/s, the fan speeds were 1400 rpm and 2800 rpm, respectively. The comparison is done in two parts. First, a comparison is done by looking

at the axial velocity over the complete wake (marked red in Figure 2). Here, the measurements were taken in steps of 20 mm in the  $yz$ -plane. Second, the velocities for the different simulation methods are plotted along two vertical lines (marked blue). Here, the velocities were measured every 5 mm in  $z$ -direction. The uncertainty in the measurement of the velocity component in axial direction is less than 0.3 m/s.

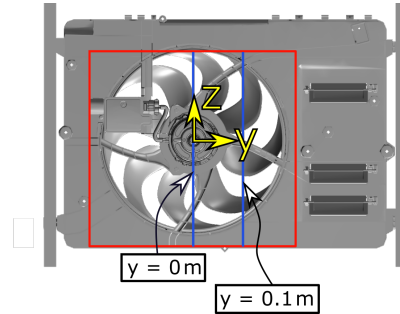


Figure 2: Investigated areas 0.04 m downstream of the fan

### Wake plane

Figure 3 shows the resulting axial velocity flow field for the three simulation methods in comparison to the experimentally obtained data. The experimental data is linearly interpolated from a grid with 20 mm steps in each direction to one with 5 mm. The CFD data is sampled with a step size of 5 mm. The higher resolution in the CFD results was necessary, to make characteristic flow features of the MRF model visible. The fan rotates counter-clockwise in this view. The hub in the center of rotation and the four struts holding it in place can clearly be identified in all pictures by the low velocities. This is also the case for the control unit (CU), that is placed in the upper left quarter and leaves a clear imprint on the wake. In the measurements, the wake of the control unit appears larger, since it was difficult to achieve proper seeding there due to the obstruction.

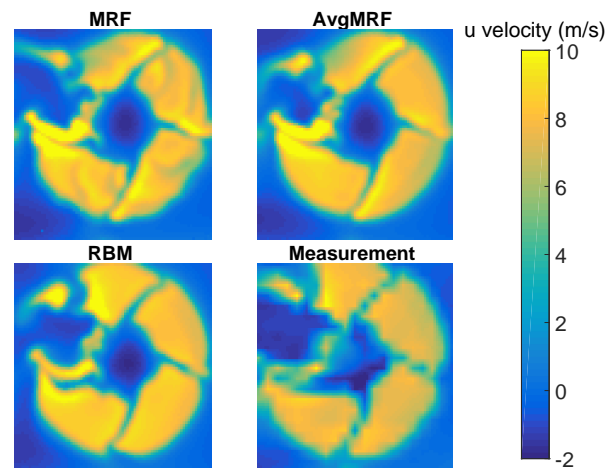


Figure 3: Axial velocity field for a rotation rate of 1400 rpm and a freestream velocity of 5 m/s

The flow field obtained by the MRF method shows the largest differences from the three simulation models compared to the measurements. The main difference is, that the flow field is disturbed by the fixed blade position, which leads to an uneven distribution. Averaging the flow field for 9 different fan positions with the average MRF approach gives a more uniform

flow field, which is comparable to the RBM simulation and the measurements.

However, there are two major differences between the MRF based simulations and the RBM simulation/measurement results. The first is an area of relatively low velocities on the top of the wake, right of the control unit. In the RBM simulation and the measurements, this area shows significantly higher axial velocities. An unsteady MRF simulation was performed to determine if this can be traced back to differences between the RANS and the URANS model. Since the URANS MRF showed the same behaviour, it is concluded, that this low velocity region is resulting from an interaction between the MRF interface and the geometry of the shroud. The reason why the other struts do not show the same effect on the flow field is, that the strut holding the control unit on top has only a distance of 4 mm to the MRF interface, while the other struts are 10 mm downstream of the interface. The second difference that is observed, is an elevated velocity behind the struts in direction of rotation for the two MRF based simulation approaches. For the RBM simulation it is hardly visible in Figure 3, but also here there are small areas with slightly elevated axial velocities. However, those areas are on both sides of the struts and of approximately equal size and magnitude. The resolution of the measurement grid is insufficient for these kinds of observations.

Figure 4 shows the same wake plane for the rotation rate of 2800 rpm. Due to the higher rotation rate, the scale had to be adjusted, but the same observations as for the 1400 rpm case can be made.

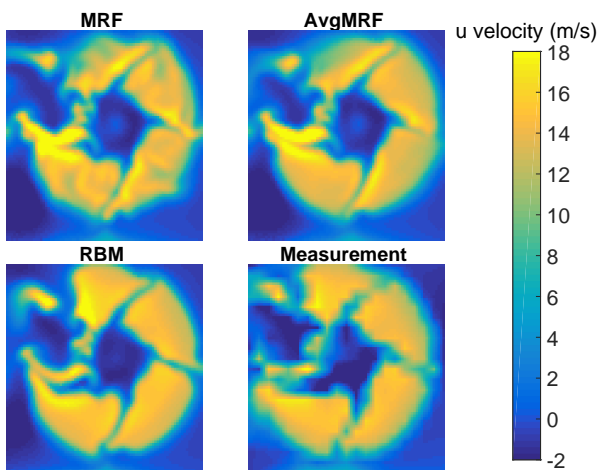


Figure 4: Axial velocity field for a rotation rate of 2800 rpm and a freestream velocity of 5 m/s

### Vertical Lines

For a closer comparison, the axial velocities along two vertical lines were plotted, one at the centerline (Figure 5) and one with a 0.1 m offset in positive  $y$ -direction (Figure 6). The measurements were repeated with a step size of 5 mm in  $z$ -direction. To facilitate the reading of the graphs, the cross-section of the fan region and the shroud is added to the plots.

Figure 5 shows the measured and simulated axial velocities along the centerline of the fan, for 1400 rpm (left) and 2800 rpm (right). Overall, all three fan modelling approaches match the experimental data relatively well for the lower rotation rate. The largest differences occur in the upper half ( $z > 120$  mm), close to the control unit. There, lower axial velocities have been observed and described in the previous section (compare Fig. 3 and 4). For the 2800 rpm case, just above the hub

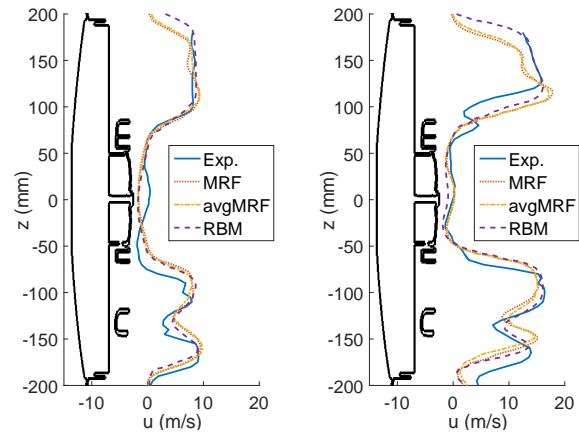


Figure 5: Axial velocity at 5 m/s for 1400 rpm (left) and 2800 rpm (right) 0.04 m behind the fan on the centerline (comp. Fig. 2)

( $90 < z < 120$  mm), the measured velocities are considerably lower than the ones obtained from the CFD simulations. Since this result was repeatable, a possible reason might be that the seeding did not reach the area. No notable difference between the MRF and the averaged MRF results can be seen along the centerline.

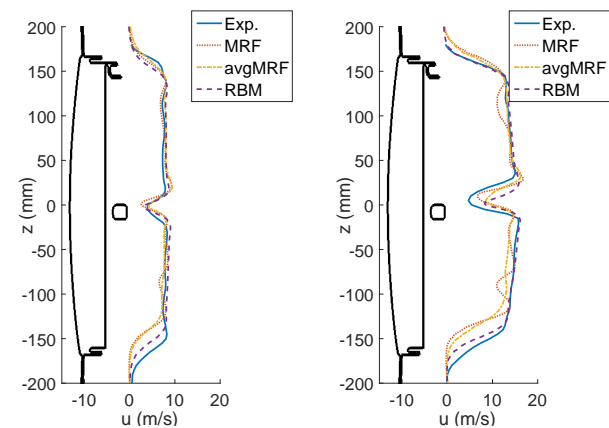


Figure 6: Axial velocity at 5 m/s for 1400 rpm (left) and 2800 rpm (right) 0.04 m behind the fan 0.1 m to the right of the centerline

Figure 6 shows the axial velocity over a vertical line that is located 0.1 m to the right of the center of rotation, as seen from the downstream view. For the 1400 rpm case (left), all simulation models agree well with the measurement data. It can be observed, that the wake for the MRF based simulations has a smaller extent in  $z$ -direction than the wake in the RBM results or the measurement data. At 2800 rpm large differences between the standard (single) MRF and averaged MRF method can be seen on both sides of the hub. The velocities for the standard MRF model are fluctuating notably. The averaging over multiple MRF simulations with different fan positions successfully removes these fluctuations and achieves a uniform flow field distribution similar to the RBM and measurement data.

## Average MRF - Increment Study

Since the first attempt of averaging the flow field obtained by multiple MRF simulations showed a notable improvement weighted with a low additional computational effort, it was decided to investigate the impact of the step size in rotation on the results. For this particular fan, the blade geometry repeats itself every 45 deg, therefore it is only necessary to cover this range. In addition to the previously presented 9 positions with a 5 deg angle increment, cases with finer (45 x 1 deg) and coarser (3 x 15 deg) increment are examined.

Figure 7 shows the wake plane 0.04 m downstream of the fan where the 45 deg range is covered by increments of 1 deg, 5 deg and 15 deg at a rotation rate of 2800 rpm. There are no visible differences between the resulting flow fields obtained by using the average over 45 MRF simulations with each 1 deg difference in fan blade position or 9 simulations with an increment of 5 deg. Similar results were also obtained when averaging over 3 x 15 deg positions. However, for this case, some small blade shadows start to re-appear.

Figure 8 shows a comparison for the same increments along the two vertical lines that were presented in the previous section. Here, an increase or decrease of averaged MRF simulations does not show any notable effect.

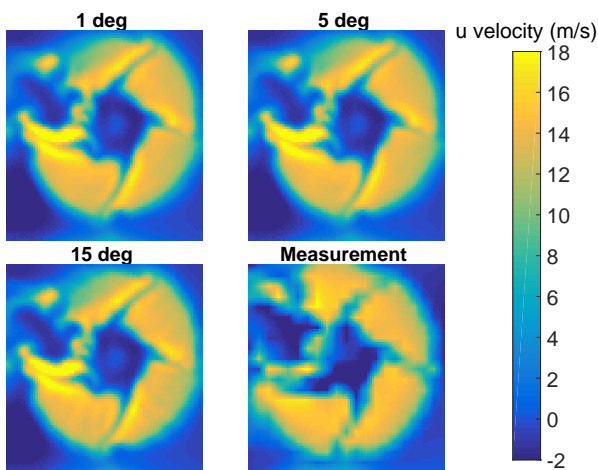


Figure 7: Wake for different angle increments

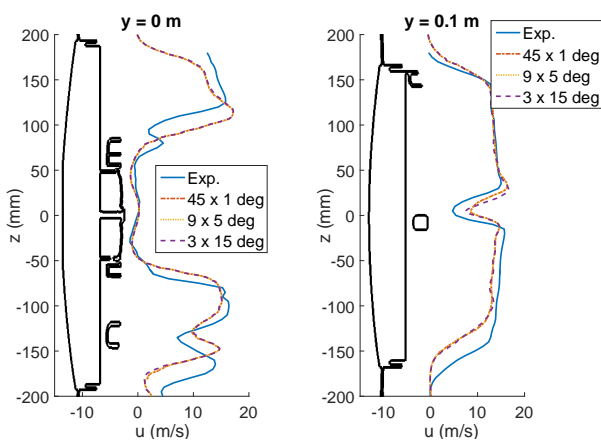


Figure 8: Axial velocity along the two vertical lines for different increments in fan blade angle compared to experimental data (5 m/s, 2800 rpm)

## Conclusions

In this paper, results comparing three different fan modelling approaches with measurement data, obtained using a 2 D LDA system, are presented. The commonly used standard Moving Reference Frame (MRF) model showed large differences to the experimental data, since the fixed blades caused an imprint in the wake and therefore an uneven flow distribution. It was shown that it is possible to cost-efficiently remove those imprints by averaging the flow field over multiple steady-state MRF simulations with different fan positions. A parametric study demonstrated that the simulation of two additional fan positions was already sufficient in the presented test set-up to substantially improve the resulting flow field. Although the Rigid Body Motion model with URANS simulation showed the best agreement with the measurement data, it also requires the largest computational effort. Hence, the proposed average MRF approach is a good alternative to the common fan modelling methods, as it gives improved results with minimal increased computational costs.

## Acknowledgements

The authors would like to thank the Volvo Car Corporation for their support in this study. We would like to especially thank David Englen for his support in the experimental work, as well as Tore Bark for many interesting discussions of the results. Furthermore, we thank the Swedish Energy Agency for the funding of this project, as well as the Swedish National Infrastructure for Computation (SNIC) for providing computational resources.

## References

- [1] P. Gullberg, L. Löfdahl, and P. Nilsson. Cooling airflow system modeling in cfd using assumption of stationary flow. In *SAE Technical Paper*, 2011.
- [2] P. Gullberg, L. Löfdahl, A. Tenstam, and P. Nilsson. 3d fan modeling strategies for heavy duty vehicle cooling installations - cfd with experimental validation. In *FISITA World Automotive Congress*, 2008.
- [3] J. Hurault, S. Kouidri, F. Bakir, and R. Rey. Experimental and numerical study of the sweep effect on three-dimensional flow downstream of axial flow fans. *Flow Measurement and Instrumentation*, 21(2):155 – 165, 2010.
- [4] G. Kergourlay, S. Kouidri, G. W. Rankin, and R. Rey. Experimental investigation of the 3d unsteady flow field downstream of axial fans. *Flow Measurement and Instrumentation*, 17(5):303 – 314, 2006.
- [5] M. Khaled, F. Mangi, H. E. Hage, F. Harambat, and H. Peerhossaini. Fan air flow analysis and heat transfer enhancement of vehicle underhood cooling system towards a new control approach for fuel consumption reduction. pages 439–450, 2012.
- [6] A. Zanon, M. D. Gennaro, H. Kuehnelt, and D. Caridi. Broadband noise of axial fans: an experimental and computational benchmark study. In *American Institute of Aeronautics and Astronautics*, pages 373–376, 2013.
- [7] F. Zenger, C. Junger, M. Kaltenbacher, and S. Becker. A benchmark case for aerodynamics and aeroacoustics of a low pressure axial fan. In *SAE Technical Paper 2016-01-1805*, 2016.